The electrochemical microbial tree: A new concept for wastewater treatment

Morgane Hoareau, Luc Etcheverry, Olivier Chapleur, Chrystelle Bureau, Cédric Midoux, Benjamin Erable, Alain Bergel

Chemical Engineering Journal 454 (2023) 140295

Contents lists available at ScienceDirect

Chemical Engineering Journal

journal homepage: www.elsevier.com/locate/cej

The electrochemical microbial tree: A new concept for wastewater treatment

Morgane Hoareau [a], Luc Etcheverry [a], Olivier Chapleur [b], Chrystelle Bureau [b], Cédric Midoux [b], Benjamin Erable [a], Alain Bergel [a,*]

[a] Laboratoire de Génie Chimique, Université de Toulouse, CNRS, INPT, UPS, Toulouse, France
[b] Université Paris Saclay, PRocédés biOtechnologiques au Service de l'Environnement, INRAE, 92761 Antony, France

ARTICLE INFO

Keywords:
Aerobic treatment
Electroactive biofilm
Microbial electrochemical snorkel
Microbial elecrochemical technology
Microbial population
Biomimicry

ABSTRACT

Most wastewater treatment plants involve activated sludge units, in which the organic matter to be removed is oxidised by aerobic microorganisms. These units are highly energy intensive because of the power consumed to force oxygen transfer to the wastewater by aeration. An innovative device is presented here; it is called the "electrochemical microbial tree (EMT)" and is based on the opposite strategy: the organic matter is drawn up from the wastewater towards the air phase by capillary action along a porous structure, which hosts the microorganisms that oxidise the organic matter.

The EMTs were made of carbon felt, with the bottom immersed in wastewater (14 cm), while the top emerged into the air at different heights (4, 8 or 12 cm). COD removal increased linearly with the height of the aerial section. The greatest height led to COD removal rates of 807 ± 62 mg O_2/L/h, i.e. 2.6 times those of the control experiments. During COD removal, the pH decreased from 7.6 to 7.4 ± 0.2 with EMTs, while it increased to 7.9 ± 0.1 in the controls. The biofilm on the immersed section developed as the height of the aerial section increased. Many electroactive species were identified in the microbial populations, belonging to the *Bacteroidia*, *Gammaproteobacteria* and *Clostridia* classes. These observations revealed that electron transfer along the conductive felt contributed to organic matter oxidation, in parallel with mass transfer by capillarity. These pioneering results present the EMT as a promising new wastewater treatment disposal system that does not require any energy input.

1. Introduction

Treating urban and industrial wastewater has become a crucial element in the protection of public health and the reduction of the environmental impact of human development [1]. Unfortunately, wastewater treatment plants (WWTPs) are extremely energy-intensive [2,3]. Electricity is their main energy source [4] and accounts for 25–50 % of the operating costs of traditional activated sludge plants [5]. It has been estimated that WWTPs represent around 1 % of the European Union's electricity consumption and up to 4 % of the USA's [5]. In the European Union, the overall energy consumption of WWTPs, approximately 27 TWh/year, is equivalent to the total annual electricity consumption of Serbia [6].

A major objective of WWTPs is to remove the organic matter contained in wastewaters, and their efficiency is assessed by the reduction of the chemical oxygen demand (COD) of the treated outlet [7]. This objective is generally attained by implementing the aerobic oxidation of the organic matter in activated sludge units. Conventional activated sludge units are one of the most widely used secondary treatment technologies [4]. This technology is well-mastered and efficient, even at very large scale, but it suffers from the high cost of supplying oxygen, because intensive aeration of wastewater is required to maintain the sludge particles in suspension, to sustain microbial growth, and to supply the microorganisms with the dissolved oxygen necessary to degrade the organic matter [8]. Energy-intensive processes, such as air bubbling, are used to enhance oxygen transfer from the gas phase (air) to the liquid phase (wastewater) [8,9]. The electric energy consumed by the aeration process is generally responsible for around half the power consumed by WWTPs and ratios of up to 75 % have been reported [9].

In the current context of compulsory energy saving, reducing the energy cost of aeration in WWTPs has become a key challenge. Intensive research is being carried out in various ways, such as improving the

* Corresponding author.
E-mail address: alain.bergel@toulouse-inp.fr (A. Bergel).

https://doi.org/10.1016/j.cej.2022.140295
Received 9 September 2022; Received in revised form 27 October 2022; Accepted 7 November 2022
Available online 11 November 2022

aeration equipment [10], refining the strategies of dissolved oxygen control [11] and even replacing air by pure oxygen [4]. Nevertheless, it is difficult to expect huge energy saving to be achieved simply by improving the existing set-ups, because the basic barrier is the low solubility of oxygen in aqueous systems.

With the objective of drastically reducing the energy cost of the biodegradation of organic compounds in WWTPs, we propose a groundbreaking concept based on exactly the opposite strategy. Oxygen is no longer transferred from the air phase to the liquid wastewater but, on the contrary, the organic matter to be oxidised is transported from the wastewater towards the air phase. This new device, which we propose to name the "electrochemical microbial tree (EMT)", consists of a three-dimensional porous structure colonised by a microbial biofilm. In operation, the bottom section of the EMT is immersed in the wastewater while the top section is exposed to the air above. The organic matter to be removed from wastewater is drawn up from the immersed section to the aerial section by capillarity and diffusion. In this upper section, the organic matter is oxidised aerobically by the microorganisms that make up the biofilm (Fig. 1.A).

Movement of the solution from the lower to the upper section is due to the dual effects of capillary rise and water evaporation on the top section exposed to air. Water evaporation from the top section of the EMT acts as the driving force of capillarity. The name of the device proposed here is derived from its similarity to the life mechanism of trees, in which water and mineral salts forming the sap are pumped from the soil and carried through the xylem to the leaves by capillary action [12,13]. In trees, this action is driven by water evaporation from the leaves.

To the best of our knowledge, this is the first time that such a device is described, following the recent granting of a patent [14]. Deploying it in WWTPs would allow drastic energy saving, because the EMT is a completely passive system, which does not require any energy supply in operation. To some extent, which remains to be assessed, the conventional activated sludge bioreactors, which require energy-intensive aeration, could be replaced by EMT systems, which are zero-cost in terms of operational energy expenditure. The purpose of this work is to present the concept, provide initial proof of efficiency and outline possible avenues for research, improvement, and development.

2. Materials and methods

2.1. Media and electrochemical microbial tree (EMT) set-up

Experiments were carried out using synthetic wastewater composed of 160 mg/L peptone, 110 mg/L beef extract, 30 mg/L urea, 28 mg/L K_2HPO_4, 7 mg/L NaCl, 4 mg/L $CaCl_2{\cdot}2H_2O$, 2 mg/L $Mg_2SO_4{\cdot}7H_2O$ and

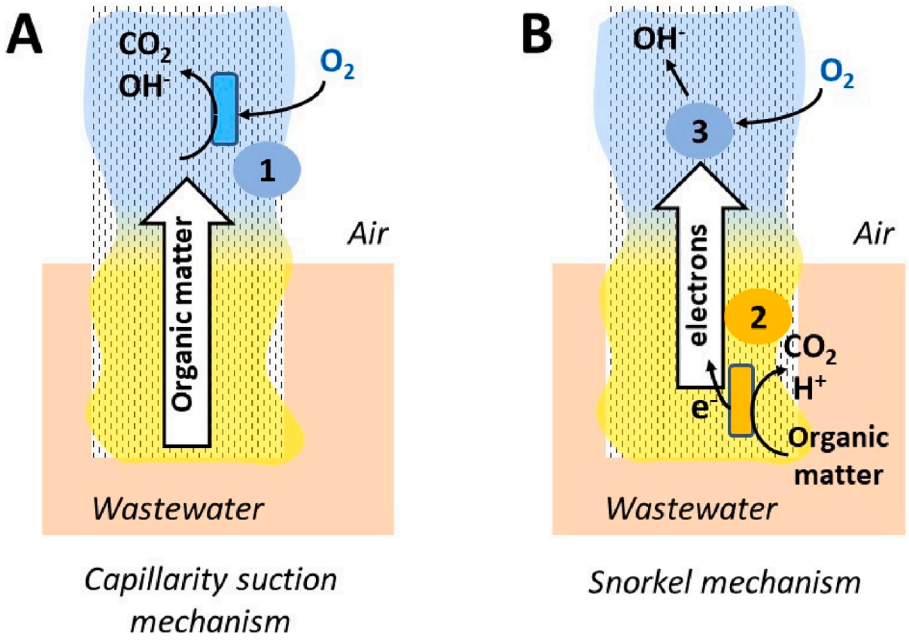

Fig. 1. The Electrochemical Microbial Tree (EMT) combines two mechanisms. The lower, immersed section is colonised by a biofilm, which is mainly anaerobic (yellow); the upper part, exposed to the air, is colonised by a biofilm, which is mainly aerobic (blue).
A) Organic matter is transported by capillarity to the upper section, where it is oxidised by aerobic microorganisms, for instance, in the case of acetate (Reaction 1):

$$CH_3COO^- + 2O_2 \rightarrow 2CO_2 + H_2O + OH^- \quad (1)$$

B) In parallel, according to the well known "microbial electrochemical snorkel" mechanism, organic matter is oxidised by the exoelectrogenic biofilm on the immersed section (Reaction 2):

$$CH_3COO^- + 2H_2O \rightarrow 2CO_2 + 7H^+ + 8e^- \quad (2)$$

and the electrons produced are transported via the conductive support to the aerial section, where they are released by the oxygen reduction reaction (Reaction 3):

$$2O_2 + 4H_2O + 8e^- \rightarrow 8OH^- \quad (3)$$

which can be catalysed abiotically or microbially.

20 mM acetate. The medium was inoculated with 5 % (v/v) of vermicompost fertiliser obtained from cattle and/or horse manure (Or Brun, France). The soluble Chemical Oxygen Demand (COD) after inoculation was around 1,28 mg O_2/L.

Experiments were carried out in vertical tube reactors, consisting of glass cylinders 37 cm high and 4.2 cm in diameter. The reactors were equipped with nozzles at each extremity to allow the solution to flow from bottom to top, while ensuring that the solution remained at a constant height of 27 cm (Fig. 1). Each vertical tube reactor was placed in a closed hydraulic loop including a single-channel peristaltic pump (Masterflex®, Cole-Parmer, USA) and a 2-L storage tank (Schott bottles). Where specified, the solution was recirculated in each loop at 1.5 mL. min^{-1}. In operation, the volume of solution remaining in the reactors was thus 350 mL.

Each reactor was equipped with an EMT structure made of two strips of carbon felt (RVG 4000, Mersen, France) 4 cm wide, 0.5 cm thick and 18, 22 or 26 cm high, assembled in a cross shape with a titanium rod (1 mm in diameter) through the centre, over the whole height (Fig. 2). Control experiments were performed using non-porous structures, which had the same cross shape and the same dimensions as the EMTs (26 cm high). In this case, each of the two sheets of the cross were composed of three superimposed plastic grids of 4 mm open mesh. The volume hindrance of this structure was similar to that of the EMT and allowed biofilm development. In contrast, the open mesh of 4 mm was too large to allow significant capillarity and the material was not conductive.

2.2. EMT formation and operation

Eight independent loops were run in parallel. Two EMTs measured 18 cm, two 22 cm and two 26 cm. Two control experiments were run using similar non-porous, non-conductive structures (plastic grids) measuring 26 cm. The first 7 days were dedicated to preparing the EMTs by letting a biofilm form over the entire structures and, hopefully, inside the porous structure. During this period, the EMTs were fully immersed in the vertical reactors and the solution was continuously recirculated.

On day 7, the 18-, 22-, and 26-cm high EMTs were adjusted so that 4, 8 and 12 cm, respectively, emerged above the free surface of the solution, meaning that the immersed section was 14 cm high for all the EMTs. Acetate was added to adjust the COD to the initial value of 1,280 mg O_2/L. On day 12, the COD was adjusted again by adding acetate, and recirculation of the solution was stopped. A batch phase lasting 43 h (Batch 1) was carried out in order to monitor the evolution of the COD in the vertical reactors as a function of time. After this 43-hour batch phase, recirculation of the solution was resumed. On day 14, the loops were emptied under nitrogen flow and refilled with fresh solutions. On day 17, the acetate concentration was adjusted again, recirculation was stopped and the COD in the vertical reactors was measured periodically for 19 h (Batch 2). After Batch 2, scanning electron microscopy (SEM) and confocal scanning microscopy were used to image the EMT biofilms, and the microbial populations of the immersed and aerial sections were analysed.

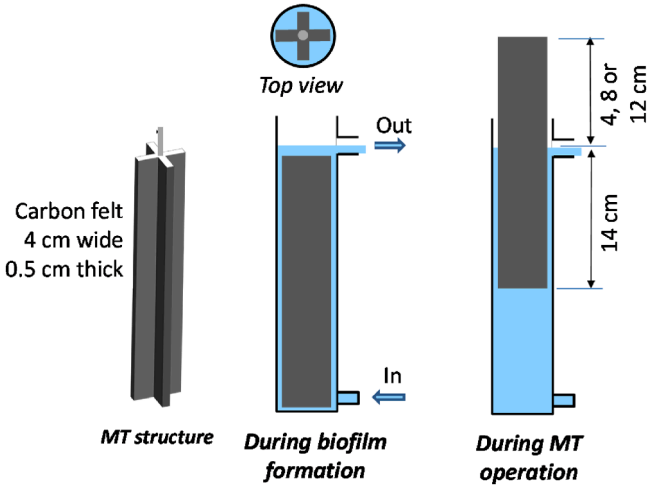

Fig. 2. Diagram of the electrochemical microbial tree (EMT). The EMT structure was made of two strips of carbon felt, 4 cm wide, 0.5 cm thick and 18, 22 or 26 cm high, assembled in a cross shape with a titanium rod (1 mm in diameter) through the centre over the whole height. The EMT structure was fully immersed in the vertical reactors during the biofilm preparation phase and was then raised by 4, 8 or 12 cm in the operation phase.

2.3. Analytical procedures and microscopy imaging

The soluble COD was measured after filtering the samples with a syringe filter (0.22 µm) using the Hach Lange LCK 314 system for concentrations ranging from 15 to 150 mg O_2.L^{-1} and LCK 514 microkits for concentrations ranging from 100 to 2,000 mg O_2.L^{-1}. Removal of the organic matter was monitored by taking successive samples from the centre of the reactors. COD removal ratios (ΔCOD) were calculated as follows:

$$\Delta\mathrm{COD}\,(\%) = \frac{COD_0 - COD_t}{COD_0}\,100 \quad (4)$$

where COD_t is the COD value at time t and COD_0 the initial value of the first sample.

SEM images (Leo 435 VP-Carl Zeiss SMT, diaphragms of 30, 50 and 700 µm) were taken after fixing, dehydrating, and plating the biofilm. Samples were immersed in a solution of 1/4 v/v phosphate buffer (0.4 M, pH 7.4), 1/2 v/v glutaraldehyde (4 % v/v) and 1/4 v/v distilled water for 20 min. They were rinsed in a solution of 1/4 v/v phosphate buffer (0.4 M, pH 7.4), 1/2 v/v saccharose (0.6 M) and 1/4 v/v distilled water in two successive 15-min steps. Samples were then successively immersed in baths of acetone 50 % (5 min), acetone 70 % (5 min), acetone 100 % (30 min), 50 % acetone + 50 % hexamethyldisilazane (HDMS) and finally 100 % HDMS until complete evaporation of the solvent. They were then coated with a gold nanolayer (10–20 nm) by cold cathode sputtering.

Confocal scanning microscopy (Axio Imager M2, light source HBO 200, filter Zeiss 09 (HP450, FT-10, LP520), Carl Zeiss, Germany) was used to image the biofilms after 10 min staining with acridine orange 0.01 % (A6014, Sigma). Two samples were collected from the immersed sections and 2 from the aerial sections of each EMT. Six different areas of each sample were imaged, meaning that 12 areas were analysed for each section of each EMT. For the EMTs with a 12-cm aerial section, only one of the two duplicates was imaged because of a technical problem. For each area imaged, a stack of n images superimposed perpendicular to the surface was made. The images were consistently 3.7 µm apart, so n was in the range of 40 to 160 images depending on the biofilm thickness. Zen software (Carl Zeiss, Germany) was used to obtain projections and determine the biofilm coverage rate of each area. The average value and standard deviation were then calculated based on the 12 areas imaged for each section of each EMT.

2.4. Molecular biology

Two samples of around 3 cm^2 were collected from the immersed sections and another two from the aerial sections of each EMT. In the case of the plastic controls, two samples were collected from the immersed sections only, because the aerial sections presented no significant biofilm development. The biofilm was collected by ultrasonication for 15 min followed by centrifugation for 15 min at 4,600 g and 6 °C. Ten mL samples of solution were also collected at mid-height in the vertical reactors: on day 14, before the solution was changed, and on day 18, at the end of the experiment. DNA was extracted using a DNeasy PowerBiofilm (Qiagen) kit, according to the manufacturer's

recommendations. High throughput 16S rRNA gene sequencing was performed at the NGS facility of the PROSE Research Unit, INRAE (Antony, France), using Personal Genome Machine (Ion Torrent™, Life Technologies, USA) technology and methods. The archaeal and bacterial hypervariable region V4-V5 of the 16S rRNA gene was amplified with the 515F (5′ -GTGYCAGCMGCCGCGGTA-3′) and 928R (5′-CCCCGY-CAATTCMTTTRAGT-3′) primers and then sequenced according to a protocol described elsewhere [15,16] with some modifications. Briefly, the V4–V5 region was amplified according to the three-step Platinum SuperFi DNA Polymerase protocol (Invitrogen). PCR products were purified using Solid Phase Reversible Immobilization (SPRI) magnetic beads (Mag-Bind TotalPure NGS magnetic beads, Omega Bio-Tek) according to the manufacturer's instructions. Purified amplicons were quantified using D1000 ScreenTape and 2200 TapeStation (Agilent Technologies). All the amplicons were then pooled in equimolar ratios to prepare the library for sequencing.

The FROGS (Find, Rapidly, OTUs with Galaxy Solution) pipeline was used to analyse the 16S rRNA tag reads. FROGS is a Galaxy workflow designed to produce a matrix of OTU abundance from in-depth sequencing amplicon data [17]. After merging the reads between 100 and 500 bp, the software was used to denoise the dataset, which was then clustered using the Swarm algorithm. Chimeras were removed with vsearch. OTUs with low abundance were removed, keeping only those representing more than 0.005 % of the whole dataset. Taxonomic affiliation was performed using Silva138 16S as a reference database. For the 44 samples sequenced, the total number of high-quality reads varied between 8,499 and 18,969, resulting in a total 838 OTUs.

A Principal Component Analysis (PCA) of all the data obtained after sequencing was performed using the mixOmics R package [18] to highlight the relationship between the samples taken in the different conditions. Low abundance OTUs were filtered out; OTUs with a frequency of more than 0.5 % in at least one sample were kept. Following this step, 174 OTUs were available for further analysis. Data were transformed by means of a centred log ratio (CLR) transformation as described in [18].

3. Results and discussion

3.1. COD removal according to the height above water

For the first 7 days, all the EMTs were fully immersed in wastewater so that a continuous microbial biofilm formed over the entire structure. On day 7, they were partly raised above the surface by 4, 8 or 12 cm, such that the immersed sections of all the EMTs were 14 cm. On day 12, the acetate concentration was adjusted to recover the initial COD value of 1,280 mg O_2/L in the reactors, recirculation of the solution was stopped, and the soluble COD was measured periodically (Batch 1, Fig. 3.A).

After 2.5 h, the highest COD removal ratio (ΔCOD) of 45 ± 3 % was achieved with the EMTs having an upper section of 4 cm above the wastewater surface. The other EMTs were less efficient, with ΔCODs of 16 ± 6 % and 24 ± 7 % for the EMTs raised by 8 and 12 cm, respectively. The control experiments displayed significantly lower removal ratios, of 13 ± 0 %. Whatever the height exposed to the air, the presence of the EMTs significantly increased the COD removal ratios.

After 43 h, at the end of Batch 1, the ΔCOD values remained the same for the controls (11 ± 1 %) and the EMTs raised by 4 cm. In contrast, they improved slightly, reaching 22 ± 3 % and 37 ± 7 %, for the EMTs raised by 8 and 12 cm, respectively. At the end of Batch 1, the pH of the controls was 7.9 ± 0.1, whereas the pH of the initial wastewater was 7.6.

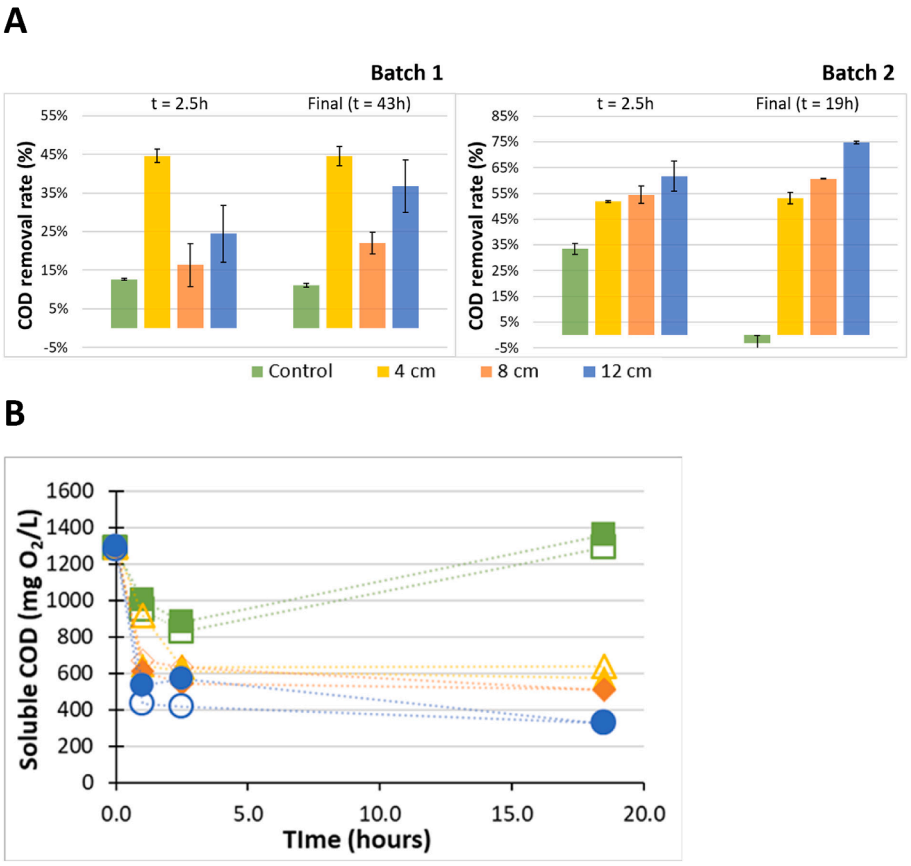

Fig. 3. COD removal. A) COD removal ratios during Batch 1 and Batch 2 after 2.5 h and at the end of the batches (43 h and 19 h for Batches 1 and 2, respectively). B) COD recorded as a function of time during Batch 2. Green: controls; yellow: EMTs with an above-water section of 4 cm; orange: EMTs with an above-water section of 8 cm; blue: EMTs with an above-water section of 12 cm. In B, the bold and empty symbols indicate duplicates.

This slight alkalinisation was consistent with the aerobic oxidation of organic matter, which produces OH^- ions, e.g. with acetate according to Reaction (1).

In contrast, the pH values of the solutions were 7.5 ± 0.2, 7.2 ± 0.3 and 7.0 ± 0.1 for the EMTs raised by 4, 12 and 8 cm, respectively. The efficiency of the EMTs as regards COD removal decreased in the same order: 4 cm above water greater than 12 cm above water greater than 8 cm above water, i.e. as the pH values decreased. It can consequently be hypothesised that the acidification of the solutions due to the presence of the EMTs actually affected the performance. In addition, the decrease in pH in the solution loop during the 12 days of operation before the start of Batch 1 may also have affected the efficiency of the EMTs. The phase of biofilm formation may have been detrimental to the subsequent operation of the system.

Consequently, at the end of Batch 1, on day 14, it was decided to replace the solution in the loops with fresh wastewater, in order to perform Batch 2 without the possible impact of the biofilm formation phase. Recirculation was resumed during 3 days in order to allow the system to cope with the disturbance caused by the total change of solutions. In particular, during this period, oxygen that was unavoidably introduced during the solution change operations was consumed by acetate oxidation.

On day 17, acetate concentration was adjusted again to recover the initial value of COD and recirculation was stopped. Batch 2 started (Fig. 3.A). The duration of Batch 2 was reduced by 24 h in comparison to Batch 1 (19 h instead of 43 h) because Batch 1 showed that the majority of COD removal was achieved at the beginning of the batch. After 2.5 h, the ΔCOD of the controls was 33 ± 2 %, while those of the EMTs raised by 4, 8 and 12 cm attained 52 ± 0.4 %, 54 ± 3 % and 62 ± 6 %, respectively.

After 19 h, at the end of Batch 2, the ΔCOD values remained relatively constant, except in the case of the EMTs raised by 12 cm, where they reached 75 % ±1%. At the end of Batch 2, the controls displayed a negative ΔCOD value because the COD value after 19 h was higher than it was initially. The problem probably came from the inoculum consisting of 5 % (v/v) of fertiliser derived from cattle and/or horse manure, which settled at the bottom of the reactor. It contained particulate organic matter, which slowly degraded into soluble organic carbon and thereby slowly increased the soluble COD value.

The pH values at the end of Batch 2 confirmed the trends observed previously: slight alkalinisation of the controls (pH 7.9 ± 0.1) and slight acidification of the reactors equipped with EMTs, with pH values of 7.4 ± 0.2, 7.1 ± 0.0 and 7.1 ± 0.1 for the EMTs with upper sections of 4, 8 and 12 cm, respectively.

Plotting the COD values against time (Fig. 3.B) showed that removal was primarily achieved during the first hour. It was consequently logical to use the values of the first hour to assess the maximum EMT efficiency. In addition, using these values minimised disturbance due the soluble COD slowly released by the inoculum. During the first hour, the COD decreased from the initial value of 1,289 ± 7 mg O_2/L to 976 ± 36 mg O_2/L in the case of the controls and to the minimum value of 482 ± 72 mg O_2/L for the EMTs raised by 12 cm. During the first hour, the EMTs with 12 cm upper sections ensured a COD removal rate of 807 ± 62 mg O_2/L/h, whereas it was 306 ± 40 mg O_2/L/h in the case of the controls. The EMT multiplied the COD removal rate by a factor of 2.6, without any energy supply.

Plotting the COD removed as a function of the aerial section height clearly showed a proportional relationship (Fig. 4). The COD removed during the first hour increased proportionally to the height of the EMT section exposed to the air. This correlation confirmed that the upper sections of the EMTs played a major role in COD removal. When the height of the aerial section increased, the surface area of the aerobic biofilm in contact with the air increased proportionally and the consumption of organic matter in this part of the EMTs increased similarly. The proportional relationship between the height of the aerial EMT section and COD removal shows that the aerobic oxidation of the organic matter in the aerial section was the rate-limiting step. There was therefore no rate-limiting effect due to mass transfer to the aerial section by capillary action. It can be anticipated that the curve would bend and reach an asymptote if the height of the aerial section was increased far beyond 12 cm because mass transfer to the aerial section would finally become rate-limiting. Here, the curve does not bend, meaning that the EMTs with aerial sections of 12 cm did not reach maximum efficiency. COD removal could be further increased by exposing even more than 12 cm of the EMT to the air.

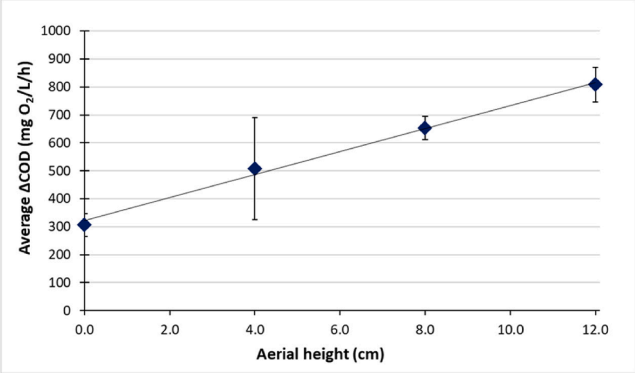

Fig. 4. COD removal as a function of the height of the above-surface section. COD removal rates (mg O_2/L/h) calculated during the first hour of Batch 2 are plotted against the height in contact with the air. The value when this height is zero is the COD removal rate measured for the control experiments. The values are the average of the duplicates.

3.2. *pH evolution shows a "microbial electrochemical snorkel" mechanism*

The aerobic oxidation of acetate should cause alkalinisation of the solution according to Reaction 1:

$$CH_3COO^- + 2O_2 \rightarrow 2CO_2 + H_2O + OH^- \quad (1)$$

This was the case in all the control experiments. On the contrary, the pH decreased in the reactors equipped with EMTs. This evolution of pH values supports the occurrence of a secondary mechanism, related to the "microbial electrochemical snorkel" principle (Fig. 1.B) [19–21]. According to this mechanism, the organic matter is oxidised by the exoelectrogenic biofilm formed on the immersed section of the EMT. Exoelectrogenic bacteria oxidise organic matter by transferring electrons to the conductive support [22]. For instance, in the case of the oxidation of acetate:

$$CH_3COO^- + 2\,H_2O \rightarrow 2\,CO_2 + 7H^+ + 8e^- \quad (2)$$

The electrons produced are transported by electric conduction along the conductive support to the top section exposed to air, where they are released to oxygen to form hydroxide ions:

$$O_2 + 4\,H_2O + 8e^- \rightarrow 8\,OH^- \quad (3)$$

A continuous biofilm and/or a continuous liquid phase in the EMT is necessary to allow ion motion between the two sections to achieve charge balance [23,24].

The microbial electrochemical snorkel principle has been successfully applied for the bioremediation of hydrocarbon-polluted marine sediments [25] and soils [26] and it has been suspected to play some role in biogeochemical cycles [27]. In the context of wastewater treatment, the principle has been mainly implemented in wetlands, with interesting results even at large scale [28]. It generally consists of filling the wetland with an electrochemically conductive bed. This ensures electron flow from the bottom to the uppermost layers of the bed, which are supplied

with dissolved oxygen. In this context, the system is called "microbial electrochemically assisted treatment wetland (METland)" [29] or sometimes "electroactive biofilm-based constructed wetland (EABB-CW)" [30].

According to the microbial electrochemical snorkel mechanism, the pH of the immersed section should decrease (Reaction 3), as observed in all the reactors equipped with EMTs. Consequently, the observed pH evolution strongly suggests occurrence of this mechanism thanks to the conductive properties of the carbon felt used as the porous structure of the EMTs. Furthermore, it is a well-known fact that acidification of electroactive biofilms inhibits their exoelectrogenic capacity [24,31,32]. Here, the decrease in pH can explain the waning of the EMT effectiveness after a few hours.

Acidification could also be the cause of the reduced performance observed in Batch 1, which was carried out after the EMTs had been running for 12 days in closed loops, without prior replacement of the solutions. It should be mentioned that the changes in pH remained moderate (from 7.6 to 7.0) because they were measured in the bulk of the solutions. The decrease in the pH of the solutions was the result of proton transfer from the biofilms. The pH values within the biofilms can consequently be expected to be significantly lower.

3.3. Biofilm imaging

SEM images showed dense microbial clusters on the carbon fibres of the immersed sections of the EMTs, while colonisation was sparser on the sections exposed to the air (Fig. 5.A). Actually, the steps required to prepare the surface for SEM imaging can disturb the structure of the biofilms and it would therefore not be advisable to draw conclusions about the fine structure of the films. However, the many images taken showed that the biofilms formed around the fibres were never thick enough to present a risk of clogging the felt porosity. In these conditions, it can be said that, as expected, the biofilm in and on the EMTs was more like a surface coating around the fibres than a thick structure within the pores of the felt.

Images obtained by confocal scanning microscopy showed substantial differences in the biofilm coverage ratios from one imaged area to another (12 areas were analysed for each section of each EMT). However, the general trend displayed low biofilm coverage on the sections exposed to the air, with biofilm coverage ratios from 8 ± 8 % (4 cm exposed) to 13 ± 12 % (12 cm exposed), which did not depend significantly on the exposed height (Fig. 5.B).

In contrast, for the immersed section, the biofilm coverage ratio varied proportionally to the height of the exposed section, from 14 ± 6 % when only 4 cm were exposed to 25 ± 7 % when 12 cm were exposed. The height of the upper section directly affected the development of the biofilm on the immersed section. A larger surface area exposed to the air promoted the development of the biofilm on the immersed section.

This observation is another argument supporting the microbial electrochemical snorkel mechanism. The exoelectrogenic species that grew on the bottom section of the EMTs (the anode part of the snorkel), released the electrons resulting from their respiration metabolism to the conductive felt. In the absence of electron acceptors in solution, oxygen for instance, they "respired" the conductive carbon felt, hence their initial name of "anode-respiring bacteria" [22]. If electrons produced by the bacteria were not released from the felt structure, its potential would decrease to the point of prohibiting the bacteria from continuing to release their electrons to the support. Bacterial development and survival would no longer be possible. The extraction of electrons from the conductive support is essential for the microbial development.

When the height of the aerial section increased, the surface area in contact with the air increased proportionally and the electron flow extracted from the felt structure increased in the same proportion. The aerial section was the cathode of the snorkel. The larger the upper section, the greater the electron flow extracted from the immersed section. The exoelectrogenic bacteria could therefore grow more quickly on the submerged part. The microbial biofilm developed more abundantly when the upper section had a larger surface area and was thus able to extract more electrons (Fig. 1.B).

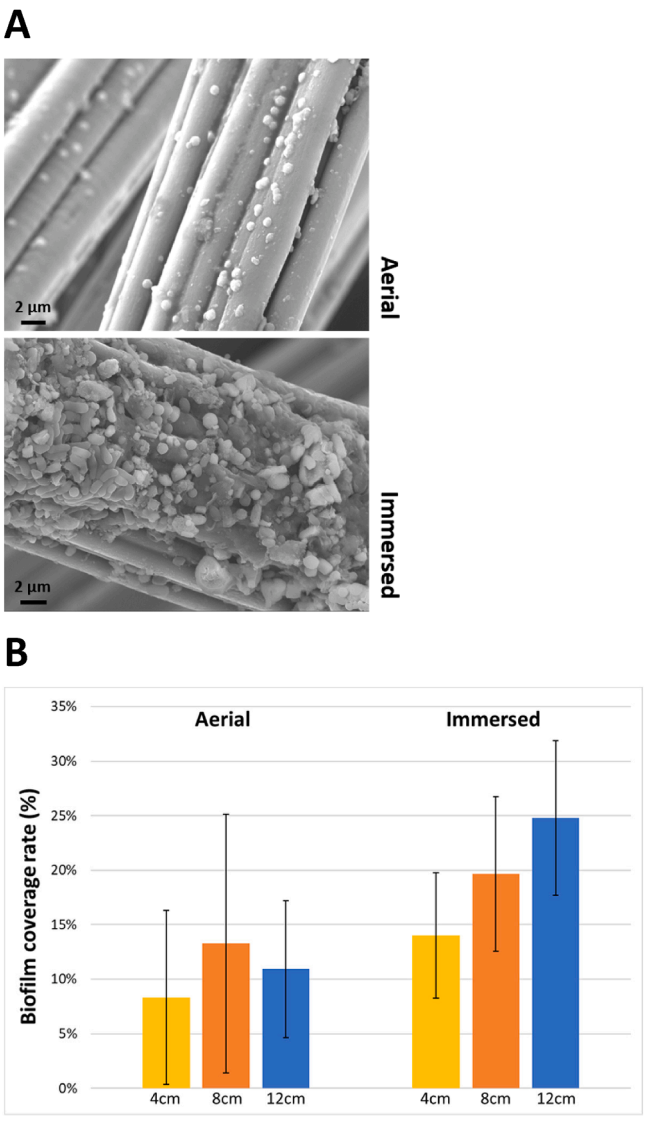

Fig. 5. Biofilm coating. A) Representative SEM images showing a denser microbial colonisation of the fibres on the immersed section of the EMT structure. B) Biofilm coating ratios extracted from images obtained by confocal scanning microscopy for both the above-water and immersed sections. Each value is an average based on the analysis of 24 images (6 spots imaged on two different samples for each section of each duplicate) for the EMTs with 4-cm and 8-cm sections above water. Due to a technical problem, only 12 images were analysed for the EMT with a 12-cm section exposed to the air.

3.4. Microbial population analysis

The microbial populations of both the immersed and aerial biofilms were analysed. Two samples were collected from each section of each EMT. In the case of the controls, samples were collected only on the immersed sections, because the aerial sections were not sufficiently colonised. Microbial populations were also analysed in the solutions on day 14 (before changing the solution) and on day 18 (the end of the experiment). Sequencing data were first examined at class level (Fig. 6). Samples displayed a total of 838 OTUs belonging to six major classes: *Bacilli, Bacteroidia, Gammaproteobacteria, Clostridia, Alphaproteobacteria* and *Negativicutes*.

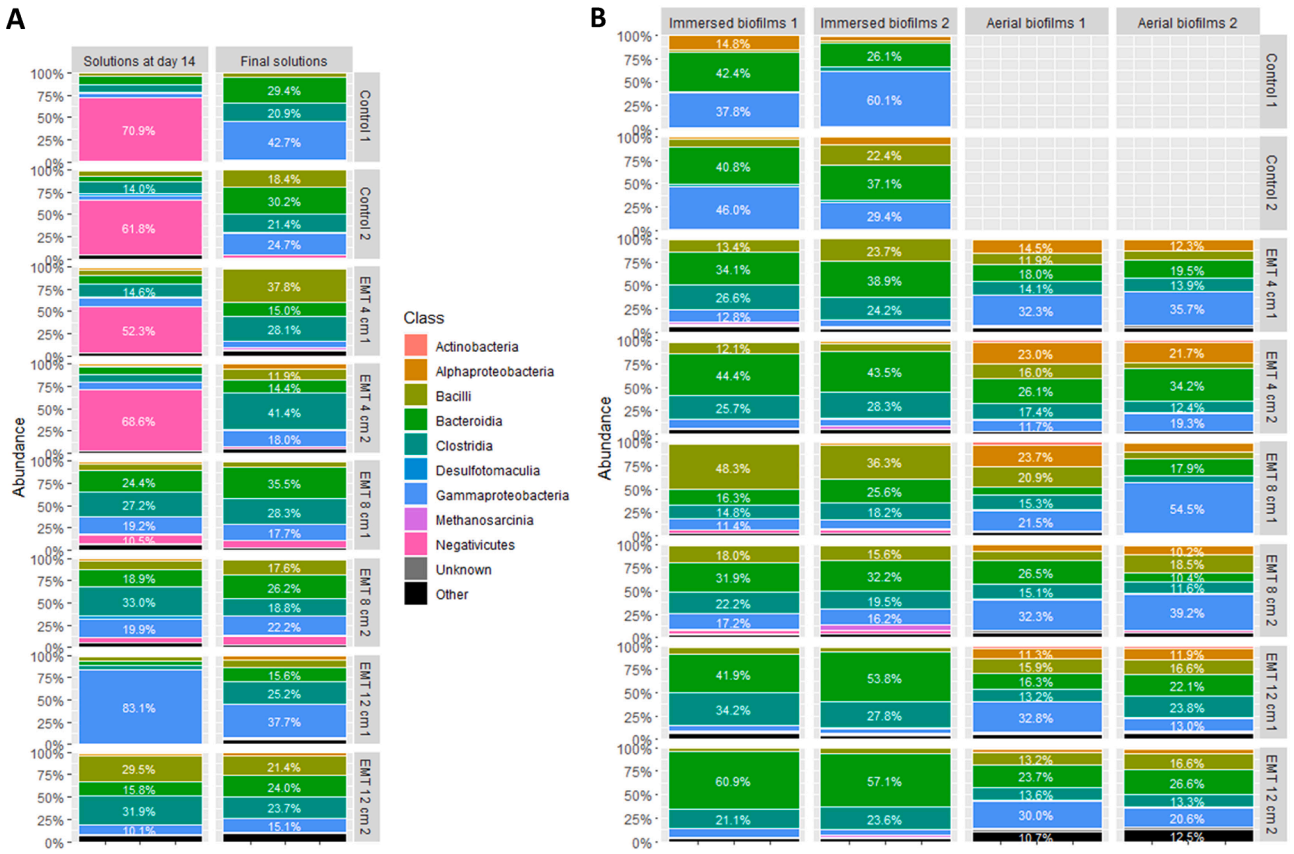

Fig. 6. Microbial populations of the solutions and EMT biofilms at class level. The percentages give the relative abundances of the classes. A) In solution, Column 1: solution samples collected on day 14, before solution replacement; Column 2: solution samples collected at the end of the experiment; B) In biofilms: Columns 1 and 2: the two samples collected from the immersed biofilm; Columns 3 and 4: the two samples collected from the aerial biofilm (no such biofilm samples were taken for the controls because the biofilm was too thin for an analysis to be attempted). The lines correspond to the different EMTs, each in duplicate (numbered "1″ and "2").

166 OTUs belonged to *Bacilli* (*Firmicutes* phylum). This class was very little present in the solutions on day 14 but it was found in all samples, both biofilms and solutions, at the end of the experiment, with a relative abundance of 11 ± 4 % to 30 ± 16 %, except in the case of one of the plastic controls. Forty-two of these OTUs were of the *Bacillus* genus, which is known to contain electroactive species [33].

The *Bacteroidia* class (*Bacteroidota* phylum) was also present in all samples but in greater abundance, from 27 ± 7 % to 53 ± 8 %, in the immersed biofilms. Among the 74 OTUs of this class and the 21 class-affiliated genera, 16 belonged to the *Lentimicrobium* genus (48 ± 1 % for the 12-cm-exposed EMTs) and 5 to the *Cloacibacterium* genus. These facultative anaerobic bacteria accept both oxic and anoxic environments, are electroactive, and are commonly involved in the degradation of organic compounds [34–37].

Gammaproteobacteria (94 OTUs) were present in all samples, except in the solutions on day 14. This class was the most prevalent in all the plastic controls (34 ± 13 % in solutions, 43 ± 13 % in the biofilms) and in one 12-cm-exposed EMT (83 %). For the other EMTs, the relative abundance of this class was 29 ± 12 % in the upper section biofilms and 10 ± 16 % in the immersed biofilms. The main genus was *Pseudomonas* in the biofilms and *Acinetobacter* in the solutions. Both genera have been described as hosting electroactive bacteria able to perform extracellular electron transfer in aerobic conditions [36].

259 OTUs were affiliated to the *Clostridia* class. Its relative abundance remained low in biofilms: 14 ± 4 % and 24 ± 5 % in the aerial and immersed biofilms, respectively. The class was more present in the solutions (20 ± 11 % and 26 ± 7 % on days 14 and 18). The two major genera in this class were *Sedimentibacter* and *Sporacetigenium*.

The *Negativicutes* class (*Firmicute* phylum) was the most prevalent in several samples on day 14 (66 ± 6 % and 60 ± 12 % for the solutions of the control reactors and the solutions of the 4-cm-exposed EMTs, respectively). Its relative abundance then dropped to less than 10 % in all samples at the end of the experiment.

Alphaproteobacteria were detected (63 OTUs) in the aerial biofilms only, with a relative abundance that decreased as height increased: 18 ± 5 %, 13 ± 7 % and 9 ± 4 % for upper section heights of 4, 8 and 12 cm, respectively. The *Brevundimonas* genus was predominant. Some *Brevundimonas* species have been described as being capable of extracellular electron transfer [38]. The exposed height did not have a significant impact on the microbial populations, except in the case of the *Alphaproteobacteria* class.

The immersed and aerial biofilms displayed significant differences in their microbial populations. The Principal Component Analysis (PCA) confirmed this trend (Fig. 6). Component 1, accounting for 28 % of the variance, distinguished the exposed and immersed biofilms. Component 2, accounting for 16 % of the variance, determined whether the samples came from the solutions (on day 14 and at the end of the experiment) or from the biofilms. The PCA therefore revealed four groups: samples taken from solutions, biofilms taken from the aerial sections of the EMTs, biofilms taken from the immersed sections of the EMTs, and biofilms taken from the immersed sections of the controls. No biofilm samples were taken from the upper section of controls because the biofilms were too thin and the amount of DNA collected was insufficient for analysis. Interestingly enough, according to component 2, the biofilms from the EMTs were gathered on one side, while the biofilms from the controls and the solutions were on the other.

Correlation circles associated with the PCA score plot showed which OTUs were mainly responsible for the ordination of the samples in the

previously described groups (Fig. 7). They confirmed the observations made with abundance histograms. In particular, the OTUs in the solutions on day 14 were specific to the *Negativicute* class. Consequently, this class, whose abundance then decreased, did not play a crucial role in the efficiency of the EMT measured in Batch 2. *Alphaproteobacteria* and *Gammaproteobacteria* were characteristic of the biofilm samples taken from the aerial sections of the EMTs and of the biofilms sampled from the immersed sections of the controls. *Bacilli* were characteristic of the emerged biofilms. *Bacteroidia* and *Clostridia* were mainly found in the immersed biofilms of the EMTs and in solutions.

To sum up, the microbial populations of the immersed and aerial biofilms differed significantly. The nature of the support (plastic controls vs carbon-felt EMTs) also clearly affected both the quantity of biofilm and the nature of the microbial populations. As the final remark on this section, it should be emphasized that three of the most abundant classes present in the immersed biofilms – *Bacteroidia*, *Gammaproteobacteria* and *Clostridia* – had previously been found in exoelectrogenic biofilms subjected to intense periodic aeration [36]. In particular, four of the genera identified here – *Cloacibacterium*, *Pseudomonas*, *Acinetobacter* and *Brevundimonas* – were also present in bidirectional biofilms, i.e. biofilms able to sustain both exoelectrogenic and electrotrophic behaviours [36]. Such development of numerous bacterial classes and genera known to host electroactive species is another argument in favour of the occurrence of the microbial electrochemical snorkel mechanism.

3.5. Mass transfer vs Electron transfer?

Two different mechanisms can be put forward to explain why EMTs enhance COD removal. Initially, it was thought that the organic matter was drawn up from the solution to the upper, aerobic section of the EMT, where it was oxidized by aerobic microorganisms, which were supplied with oxygen coming from the air (Fig. 1.A). This mechanism corresponds to mass transfer of the organic matter from the anaerobic, lower EMT section towards the upper section exposed to the air. A comparison of the COD removal rates obtained with the EMTs vs the plastic controls supports this mechanism. The plastic grids did not provide the porous capillary structure necessary to draw up the organic matter and did not support any significant biofilm development on their upper, aerobic section. Consequently, they systematically achieved significantly lower COD removal rates.

On the other hand, the pH of the solution decreased in the presence of the EMTs, the biofilm development on the lower EMT section depended on the height of the upper section and numerous electroactive species were identified in the biofilm. All these elements consistently support the occurrence of a microbial electrochemical snorkel mechanism. This mechanism is supported by electron transfer from the lower EMT section to the upper section through the conductive support.

The impact of the snorkel mechanism can be assessed by calculating the related current density. The EMTs with an aerial section of 12 cm ensured a COD removal rate of 807 ± 62 mg O_2/L/h, where it was 306 ± 40 mg O_2/L/h for the controls. The COD removal rate achieved by the EMTs was consequently 501 mg O_2/L/h. If it had been entirely due to the snorkel mechanism, the current (I) produced would have been:

$$I = \frac{0.5VnF}{3600M_{O2}} \quad (5)$$

where 0.5 g O_2/L/h is the COD removal rate, V is the volume of solution, n = 4 is the number of electrons required to reduce one O_2 molecule, F = 96,485C/mole e^- is the Faraday constant and M_{O2} = 32 g is the oxygen molar mass. The volume of solution in the vertical reactors was 350 mL minus the volume taken up by the 14 cm of the aerial section of the EMT, i.e. 0.297 L. The COD removal rate of 0.5 g O_2/L/h corresponded to a current of 0.5 A.

The surface area of the 14-cm immersed section of an EMT was 196 cm^2. The current density due to COD removal related to the immersed surface area would consequently be 25.5 A/m^2. This value is in the range

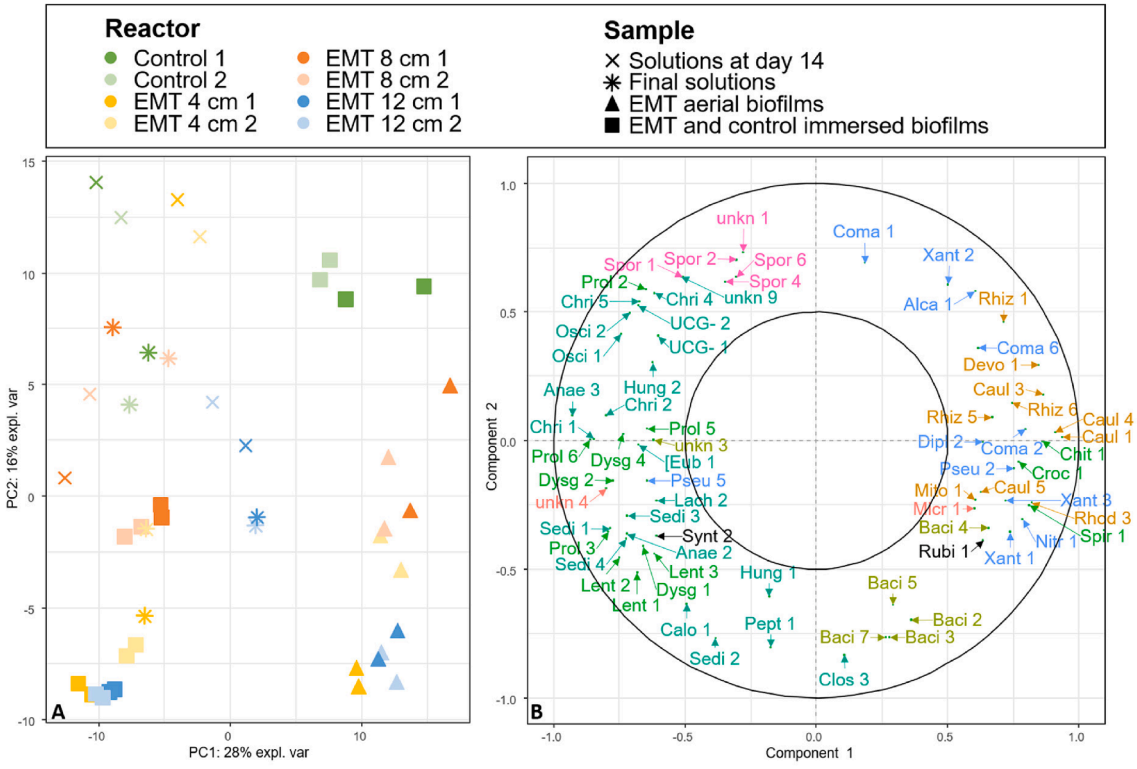

Fig. 7. PCA analysis of the microbial populations based on biofilm location (immersed or aerial) and biofilms vs solution. The "1" and "2"numbers refer to duplicates. A) Score plot of the samples B) Correlation circle. OTUs on the correlation circles are named and coloured according to the colour chart used in Fig. 6.

of the highest current densities reported in the literature for microbial anodes of similar porosity in optimal conditions, i.e. with an applied potential in controlled electrochemical set-ups [39,40]. A spontaneous process such as the snorkel mechanism cannot be expected to generate such a high current density.

Furthermore, the value of 0.5 A of current would imply that the electron flow from the lower to the upper section, through the EMT cross-section of 3.75 cm^2, corresponded to a current density of 1,300 A/m^2. This current density is related to the current that would flow along the carbon felt from the cathode section to the anode section (by definition, direction of the current is opposite to the direction of electrons). This value is incredibly huge in the context of microbial electrochemical technologies.

Actually, it is not possible to directly measure the current that flows between the anode and cathode sections of an EMT, or of any other type of application of the microbial electrochemical snorkel concept, because anode and cathode are not separated and there is no external circuit in these systems. The short-circuited anode and cathode sections are not distinguished and they can vary during system operation. Nevertheless, a specific device has been implemented recently to evaluate such currents in large scale constructed wetlands equipped with electroconductive beds [41]. The current densities were always evaluated at less than 0.3 A/m^2 [29].

If the microbial electrochemical snorkel mechanism was responsible for the entire COD removal here, the cross-sectional current density flowing along the EMT should be 1,300 A/m^2. The values evaluated in the literature for comparable systems are not above 0.3 A/m^2. This comparison unambiguously shows that the snorkel mechanism was far from being able to perform the entire COD removal. Both suction and snorkel mechanisms coexisted, probably with suction as the highly predominant mechanism.

3.6. Future research directions

Pioneering experiments have been presented here to describe the concept of the electrochemical microbial tree. The system was designed to promote the suction of the organic matter from wastewater to an upper EMT section exposed to air, where it was oxidised. Here, several consistent observations show the concomitant occurrence of a microbial electrochemical snorkel mechanism that contributed to COD removal. Distinguishing the contribution of each mechanism would be an interesting fundamental challenge. It would require a comparison of the performance of two identical structures, one conductive and the other not. However, it seems very difficult to find a non-conductive felt having the same structure as the carbon felt used in this initial study. Furthermore, the two structures should have the same surface properties, because the capillarity phenomena depend directly on the surface characteristics. It can be guessed that the precise distinction between the two mechanisms will remain a fundamental challenge for a long time.

When compared to the rates achieved in the aerobic units of current wastewater treatment plants, the maximum COD removal rate of 807 ± 62 mg O_2/L/h may seem modest. However, two points need to be emphasised here. First, EMTs are passive devices, which do not require any energy input, thus suggesting massive savings compared to aerated units. Such a huge advantage may well make a weaker performance more acceptable. Second, the pioneering experiments presented here are innovative, so there may be considerable room for improvement. For example, it was observed that the COD removal rate increased with the height of the aerial section. Fig. 4 shows that the upper performance limit was not reached and that it would be sufficient to increase the height of the aerial section to further increase the COD removal rate.

In addition, these ground-breaking results open up a wide field of research, in biomimicry in particular. The EMT concept is similar to the mechanism trees use to carry sap from their roots to their leaves, in which water transpiration acts as the driving force. The sap rises through the capillary structure of the xylem to reach the leaves of the tree, where it is enriched with compounds produced by photosynthesis. It then flows down the central structure called the phloem [12,13]. This type of passive two-way circulation could be very beneficial in the EMT system, in order to balance the pH of the biofilm between the above-water aerobic section and the immersed anaerobic section. The hydraulic architecture of trees [42] allows this circulation to take place over heights of several dozen metres. The xylem/phloem capillary structure could therefore be a powerful source of inspiration for improving EMTs.

Ideally, the biofilm should coat the largest possible inner and outer surface areas of the porous structure but it should not clog the capillaries of the structure. Keeping pores filled with the liquid phase should ensure that the organic matter can be drawn up by capillarity and diffusion through the EMT. In addition, open pores in the upper section should allow the biofilm in the above-water section to be exposed to air. Actually, the ubiquity of the sap capillary rise process in plants, including those living in mud (e.g. rice) and the most complex environments (e.g. mangrove swamps), gives good hope that it will be possible to design EMTs that are stable over time. In particular, the architecture of plant matrices can be taken as inspiration to avoid capillary clogging, which does not occur in plants, except in the context of severe hydraulic stress, due to the formation of gas bubbles by cavitation [43,44]. Similarly, drying out may be a problem for long-term operation of EMTs. We observed that partial drying out had occurred on the aerial section of some EMTs at the end of the three week experiment. This drying can be mitigated by immersing the EMT in solution for a few hours. A specific study of this point will be undertaken.

According to the reactional scheme above, acidification of the bottom section (Reaction 3) may be balanced by alkalinisation of the top section (Reaction 4). For this purpose, ion motion between the two sections should be encouraged by an adequate choice of porosity in order to optimise biofilm coating while keeping a sufficient portion of the porosity filled by the liquid phase. The extracellular polymeric substances that constitute the biofilm matrix are known to considerably enhance ion binding and accumulation [45]. SEM images showed only thin biofilms on the felt fibres (Fig. 5). Consequently, it should be pertinent to encourage a higher level of biofilm development inside the felt structure than those observed here, in order to increase the film's ionic conductivity, promote ion motion and thus favour pH balance between the upper and lower sections. This is another key area of progress for the future. In this context, it will be important to measure the pH within the biofilms to gain a better understanding of the processes at work in EMTs.

The many studies performed on the hydraulic architecture of trees should provide a good reservoir of ideas for scaling-up efficient EMTs [46]. In addition, the emerging concept of artificial trees created for seawater and brackish water desalination could also serve as a basis for EMT development on a large scale [47]. Scaling up to large scale could also take advantage of the work achieved on microbial electrochemically assisted treatment wetland (METland) [28,30,41]. METlands are constructed by simply replacing the electrically inert bed, most often gravel, used in conventional wetlands, by an electrically conductive bed, generally made of conductive granules, e.g. biochar. Some major objectives in designing METlands are similar to those of the EMT concept: to elaborate a 3-dimensional electrochemical structure, stable over time, which avoids clogging and promotes the development of a microbial biofilm that is suitable to reduce COD. Following this analogy, a large-size EMT may take a very simple design, as a porous, 3-dimensional conductive bed, which could be compared to a METland, but with the upper part exposed to the air. On this useful basis, great efforts remain to be made to design the appropriate porosity architecture, following the objectives and guidelines suggested above, because the idea of capillarity to draw up the organic matter and balance the pH gradient is not present in the METland concept.

4. Conclusion

The EMT concept has been described here and checked experimentally for the first time. The system applied to synthetic wastewater was found improve the maximum COD removal rate by a factor of 2.6 compared to controls not equipped with the EMT. The pH of the wastewater decreased during COD removal, whereas it had been expected to increase. Also surprisingly, the biofilm on the immersed EMT section developed as the height of the aerial section increased. These observations revealed the occurrence of a microbial electrochemical snorkel mechanism that contributed to COD removal. This mechanism was confirmed by the presence of many electroactive species in the microbial population of the biofilms.

These pioneering experiments have revealed many areas for improvement. For instance, pH has been shown to play a crucial role and controlling its distribution along the EMT should be an important way of optimising its structure. Avenues for improvement have been suggested in the previous section, in particular through a biomimicry strategy inspired by the hydraulic architecture of trees. The EMT is a completely passive device requiring no energy input. It can be designed very simply, as a conductive porous bed with the upper part exposed to the air. It should consequently be easily scalable to the large sizes required for wastewater treatment units. The concept should open up a promising avenue for significantly decreasing the energy cost of wastewater treatment.

Declaration of Competing Interest

The authors declare the following financial interests/personal relationships which may be considered as potential competing interests: Morgane HOAREAU has patent #FR 22 04472 issued to co-inventor. Luc ETCHEVERRY has patent #FR 22 04472 issued to co-inventor. Benjamin ERABLE has patent #FR 22 04472 issued to co-inventor. Alain BERGEL has patent #FR 22 04472 issued to co-inventor.

Data availability

Data will be made available on request.

Acknowledgements

We are grateful to the INRAE MIGALE bioinformatics facility (MIGALE, 2020) for providing support, computing, and storage resources. We express our grateful thanks to Marie-Line de Solan (LGC) for her precious help in SEM imaging.

Funding sources

This work was supported by the French *Agence Nationale de la Recherche* (ANR), within the framework of the Biotuba project (ANR17-CE06-0015).

References

[1] M. Molinos-Senante, R. Sala-Garrido, A. Iftimi, Energy intensity modeling for wastewater treatment technologies, Sci. Total Environ. 630 (2018) 1565–1572, https://doi.org/10.1016/j.scitotenv.2018.02.327.

[2] D. Fang, B. Chen, Linkage analysis for the water–energy nexus of city, Appl. Energy 189 (2017) 770–779, https://doi.org/10.1016/j.apenergy.2016.04.020.

[3] S. Longo, B.M. d'Antoni, M. Bongards, A. Chaparro, A. Cronrath, F. Fatone, J. M. Lema, M. Mauricio-Iglesias, A. Soares, A. Hospido, Monitoring and diagnosis of energy consumption in wastewater treatment plants. A state of the art and proposals for improvement, Appl. Energy 179 (2016) 1251–1268, https://doi.org/10.1016/j.apenergy.2016.07.043.

[4] G. Skouteris, G. Rodriguez-Garcia, S.F. Reinecke, U. Hampel, The use of pure oxygen for aeration in aerobic wastewater treatment: A review of its potential and limitations, Bioresour. Technol. 312 (2020), 123595, https://doi.org/10.1016/j.biortech.2020.123595.

[5] M. Gandiglio, A. Lanzini, A. Soto, P. Leone, M. Santarelli, Enhancing the Energy Efficiency of Wastewater Treatment Plants through Co-digestion and Fuel Cell Systems, accessed February 25, 2022, Front. Environ. Sci. 5 (2017), https://www.frontiersin.org/article/10.3389/fenvs.2017.00070.

[6] D. Torregrossa, G. Schutz, A. Cornelissen, F. Hernández-Sancho, J. Hansen, Energy saving in WWTP: Daily benchmarking under uncertainty and data availability limitations, Environ. Res. 148 (2016) 330–337, https://doi.org/10.1016/j.envres.2016.04.010.

[7] Y.J. Chan, M.F. Chong, C.L. Law, D.G. Hassell, A review on anaerobic–aerobic treatment of industrial and municipal wastewater, Chem. Eng. J. 155 (2009) 1–18, https://doi.org/10.1016/j.cej.2009.06.041.

[8] J. Drewnowski, A. Remiszewska-Skwarek, S. Duda, G. Łagód, Aeration Process in Bioreactors as the Main Energy Consumer in a Wastewater Treatment Plant, Review of Solutions and Methods of Process Optimization, Processes 7 (2019) 311, https://doi.org/10.3390/pr7050311.

[9] L. Åmand, G. Olsson, B. Carlsson, Aeration control – a review, Water Sci. Technol. 67 (2013) 2374–2398, https://doi.org/10.2166/wst.2013.139.

[10] M.R. Mukandi, M. Basitere, B.I. Okeleye, B.S. Chidi, S.K.O. Ntwampe, A. Thole, Influence of diffuser design on selected operating variables for wastewater flotation systems: a review, Water Pract. Technol. 16 (2021) 1049–1066, https://doi.org/10.2166/wpt.2021.061.

[11] D. Li, M. Zou, L. Jiang, Dissolved oxygen control strategies for water treatment: a review, Water Sci. Technol. 86 (2022) 1444–1466, https://doi.org/10.2166/wst.2022.281.

[12] H.R. Brown, The Theory of the Rise of Sap in Trees: Some Historical and Conceptual Remarks, Phys. Perspect. 15 (2013) 320–358, https://doi.org/10.1007/s00016-013-0117-1.

[13] M. Tyree, F. Ewers, The Hydraulic Architecture of Trees and Other Woody-Plants, New Phytol. 119 (1991) 345–360, https://doi.org/10.1111/j.1469-8137.1991.tb00035.x.

[14] A. Bergel, M. Hoareau, B. Erable, L. Etcheverry, T. Bouchez, Y. Fayolle, S. DaSilva, Procédé d'oxydation de matières organiques contenues dans un milieu liquide, Patent FR2202106, INPT-INRAE-6TMIC Ingénieries-UPS-CNRS, March 2022.

[15] C. Madigou, K.-A. Lê Cao, C. Bureau, L. Mazéas, S. Déjean, O. Chapleur, Ecological consequences of abrupt temperature changes in anaerobic digesters, Chem. Eng. J. 361 (2019) 266–277, https://doi.org/10.1016/j.cej.2018.12.003.

[16] S. Poirier, E. Desmond-Le Quéméner, C. Madigou, T. Bouchez, O. Chapleur, Anaerobic digestion of biowaste under extreme ammonia concentration: Identification of key microbial phylotypes, Bioresour. Technol. 207 (2016) 92–101, https://doi.org/10.1016/j.biortech.2016.01.124.

[17] F. Escudié, L. Auer, M. Bernard, M. Mariadassou, L. Cauquil, K. Vidal, S. Maman, G. Hernandez-Raquet, S. Combes, G. Pascal, FROGS: Find, Rapidly, OTUs with Galaxy Solution, Bioinformatics 34 (2018) 1287–1294, https://doi.org/10.1093/bioinformatics/btx791.

[18] F. Rohart, B. Gautier, A. Singh, K.-a., Lê Cao, mixOmics: An R package for 'omics feature selection and multiple data integration, PLoS Comput. Biol. 13 (2017) e1005752.

[19] B. Erable, L. Etcheverry, A. Bergel, From microbial fuel cell (MFC) to microbial electrochemical snorkel (MES): maximizing chemical oxygen demand (COD) removal from wastewater, Biofouling. 27 (2011) 319–326, https://doi.org/10.1080/08927014.2011.564615.

[20] M. Hoareau, B. Erable, A. Bergel, Microbial electrochemical snorkels (MESs): A budding technology for multiple applications. A mini review, Electrochem. Commun. 104 (2019), 106473, https://doi.org/10.1016/j.elecom.2019.05.022.

[21] B. Matturro, C. Cruz Viggi, F. Aulenta, S. Rossetti, Cable Bacteria and the Bioelectrochemical Snorkel: The Natural and Engineered Facets Playing a Role in Hydrocarbons Degradation in Marine Sediments, accessed August 29, 2022, Front. Microbiol. 8 (2017), https://www.frontiersin.org/articles/10.3389/fmicb.2017.00952.

[22] C.I. Torres, A.K. Marcus, H.-S. Lee, P. Parameswaran, R. Krajmalnik-Brown, B. E. Rittmann, A kinetic perspective on extracellular electron transfer by anode-respiring bacteria, FEMS Microbiol. Rev. 34 (2010) 3–17, https://doi.org/10.1111/j.1574-6976.2009.00191.x.

[23] M. Oliot, S. Galier, H. Roux de Balmann, A. Bergel, Ion transport in microbial fuel cells: Key roles, theory and critical review, Appl. Energy 183 (2016) 1682–1704, https://doi.org/10.1016/j.apenergy.2016.09.043.

[24] S.C. Popat, C.I. Torres, Critical transport rates that limit the performance of microbial electrochemistry technologies, Bioresour. Technol. 215 (2016) 265–273, https://doi.org/10.1016/j.biortech.2016.04.136.

[25] C.C. Viggi, E. Presta, M. Bellagamba, S. Kaciulis, S.K. Balijepalli, G. Zanaroli, M. P. Papini, S. Rossetti, F. Aulenta, The "Oil-Spill Snorkel": an innovative bioelectrochemical approach to accelerate hydrocarbons biodegradation in marine sediments, Front. Microbiol. 6 (2015) 881, https://doi.org/10.3389/fmicb.2015.00881.

[26] C.C. Viggi, M. Tucci, M. Resitano, B. Matturro, S. Crognale, V. Feigl, M. Molnar, S. Rossetti, F. Aulenta, Passive electrobioremediation approaches for enhancing hydrocarbons biodegradation in contaminated soils, Sci. Total Environ. 845 (2022), 157325, https://doi.org/10.1016/j.scitotenv.2022.157325.

[27] C.C. Viggi, B. Matturro, E. Frascadore, S. Insogna, A. Mezzi, S. Kaciulis, A. Sherry, O.K. Mejeha, I.M. Head, E. Vaiopoulou, K. Rabaey, S. Rossetti, F. Aulenta, Bridging spatially segregated redox zones with a microbial electrochemical snorkel triggers biogeochemical cycles in oil-contaminated River Tyne (UK) sediments, Water Res. 127 (2017) 11–21, https://doi.org/10.1016/j.watres.2017.10.002.

[28] A. Prado de Nicolás, R. Berenguer, A. Esteve-Núñez, Evaluating bioelectrochemically-assisted constructed wetland (METland®) for treating

wastewater: Analysis of materials, performance and electroactive communities, Chem. Eng. J. 440 (2022), 135748, https://doi.org/10.1016/j.cej.2022.135748.
[29] L. Peñacoba-Antona, C.A. Ramirez-Vargas, C. Wardman, A.A. Carmona-Martinez, A. Esteve-Núñez, D. Paredes, H. Brix, C.A. Arias, Microbial Electrochemically Assisted Treatment Wetlands: Current Flow Density as a Performance Indicator in Real-Scale Systems in Mediterranean and Northern European Locations, Front. Microbiol. 13 (2022), 843135, https://doi.org/10.3389/fmicb.2022.843135.
[30] C.A. Ramírez-Vargas, C.A. Arias, P. Carvalho, L. Zhang, A. Esteve-Núñez, H. Brix, Electroactive biofilm-based constructed wetland (EABB-CW): A mesocosm-scale test of an innovative setup for wastewater treatment, Sci. Total Environ. 659 (2019) 796–806, https://doi.org/10.1016/j.scitotenv.2018.12.432.
[31] G.-C. Gil, I.-S. Chang, B.H. Kim, M. Kim, J.-K. Jang, H.S. Park, H.J. Kim, Operational parameters affecting the performance of a mediator-less microbial fuel cell, Biosens. Bioelectron. 18 (2003) 227–334, https://doi.org/10.1016/S0956-5663(02)00110-0.
[32] F. Harnisch, U. Schröder, Selectivity versus Mobility: Separation of Anode and Cathode in Microbial Bioelectrochemical Systems, ChemSusChem 2 (2009) 921–926, https://doi.org/10.1002/cssc.200900111.
[33] B.E. Logan, R. Rossi, A. Ragab, P.E. Saikaly, Electroactive microorganisms in bioelectrochemical systems, Nat. Rev. Microbiol. 17 (2019) 307–319, https://doi.org/10.1038/s41579-019-0173-x.
[34] Y. Gao, H. Huang, C. Peng, X. Fan, J. Hu, H. Ren, Simultaneous nitrogen removal and toxicity reduction of synthetic municipal wastewater by micro-electrolysis and sulfur-based denitrification biofilter, Bioresour. Technol. 316 (2020), 123924, https://doi.org/10.1016/j.biortech.2020.123924.
[35] H. Hassan, B. Jin, E. Donner, S. Vasileiadis, C. Saint, S. Dai, Microbial community and bioelectrochemical activities in MFC for degrading phenol and producing electricity: Microbial consortia could make differences, Chem. Eng. J. 332 (2018) 647–657, https://doi.org/10.1016/j.cej.2017.09.114.
[36] M. Hoareau, B. Erable, O. Chapleur, C. Midoux, C. Bureau, A. Goubet, A. Bergel, Oxygen-reducing bidirectional microbial electrodes designed in real domestic wastewater, Bioresour. Technol. 326 (2021), 124663, https://doi.org/10.1016/j.biortech.2021.124663.
[37] M. Zheng, C. Xu, D. Zhong, Y. Han, Z. Zhang, H. Zhu, H. Han, Synergistic degradation on aromatic cyclic organics of coal pyrolysis wastewater by lignite activated coke-active sludge process, Chem. Eng. J. 364 (2019) 410–419, https://doi.org/10.1016/j.cej.2019.01.121.
[38] G. Ren, Y. Yan, Y. Nie, A. Lu, X. Wu, Y. Li, C. Wang, H. Ding, Natural Extracellular Electron Transfer Between Semiconducting Minerals and Electroactive Bacterial Communities Occurred on the Rock Varnish, Front. Microbiol. 10 (2019) 293, https://doi.org/10.3389/fmicb.2019.00293.
[39] P. Chong, B. Erable, A. Bergel, Effect of pore size on the current produced by 3-dimensional porous microbial anodes: A critical review, Bioresour. Technol. 289 (2019), 121641, https://doi.org/10.1016/j.biortech.2019.121641.
[40] M. Rimboud, D. Pocaznoi, B. Erable, A. Bergel, Electroanalysis of microbial anodes for bioelectrochemical systems: basics, progress and perspectives, PCCP 16 (2014) 16349–16366, https://doi.org/10.1039/c4cp01698j.
[41] A. Prado, Novel bioelectrochemical strategies for domesticating the electron flow in constructed wetlands, Sci. Total Environ. 735 (2020), 139522, https://doi.org/10.1016/j.scitotenv.2020.139522.
[42] P. Cruiziat, H. Cochard, T. Ameglio, Hydraulic architecture of trees: main concepts and results, Ann. For. Sci. 59 (2002) 723–752, https://doi.org/10.1051/forest:2002060.
[43] B. Choat, T.J. Brodribb, C.R. Brodersen, R.A. Duursma, R. López, B.E. Medlyn, Triggers of tree mortality under drought, Nature 558 (2018) 531–539, https://doi.org/10.1038/s41586-018-0240-x.
[44] A. Gauthey, J.M.R. Peters, M.R. Carins-Murphy, C.M. Rodriguez-Dominguez, X. Li, S. Delzon, A. King, R. López, B.E. Medlyn, D.T. Tissue, T.J. Brodribb, B. Choat, Visual and hydraulic techniques produce similar estimates of cavitation resistance in woody species, New Phytol. 228 (2020) 884–897, https://doi.org/10.1111/nph.16746.
[45] G.-P. Sheng, H.-Q. Yu, X.-Y. Li, Extracellular polymeric substances (EPS) of microbial aggregates in biological wastewater treatment systems: A review, Biotechnol. Adv. 28 (2010) 882–894, https://doi.org/10.1016/j.biotechadv.2010.08.001.
[46] M. Mencuccini, S. Manzoni, B. Christoffersen, Modelling water fluxes in plants: from tissues to biosphere, New Phytol. 222 (2019) 1207–1222, https://doi.org/10.1111/nph.15681.
[47] B. Mi, C. Finnerty, K. Conway, Prospects of artificial tree for solar desalination, Curr. Opin. Chem. Eng. 25 (2019) 18–25, https://doi.org/10.1016/j.coche.2019.06.004.